Published in final edited form as:
Cerebellum. 2010 June ; 9(2): 240–248. doi:10.1007/s12311-010-0157-x.

The Cerebellum in Children with Spina Bifida and Chiari II Malformation: Quantitative Volumetrics by Region

Jenifer Juranek,
Department of Pediatrics, Children's Learning Institute, University of Texas Health Science Center at Houston, 7000 Fannin, ste 2411, Houston, TX 77030, USA

Maureen Dennis,
Hospital for Sick Children, Toronto, ON, Canada

Paul T. Cirino,
Department of Psychology, University of Houston, Houston, TX, USA. Texas Institute for Measurement, Evaluation, and Statistics, University of Houston, Houston, TX, USA

Lyla El-Messidi, and
Department of Psychology, University of Houston, Houston, TX, USA

Jack M. Fletcher
Department of Psychology, University of Houston, Houston, TX, USA

Jenifer Juranek: Jenifer.Juranek@uth.tmc.edu

Abstract

Few volumetric MRI studies of the entire cerebellum have been published; even less quantitative information is available in patients with hindbrain malformations, including the Chiari II malformation which is ubiquitous in patients with spina bifida meningomyelocele (SBM). In the present study, regional volumetric analyses of the cerebellum were conducted in children with SBM/ Chiari II and typically developing (TD) children. Total cerebellar volume was significantly reduced in the SBM group relative to the TD group. After correcting for total cerebellum volume, and relative to the TD group, the posterior lobe was significantly reduced in SBM, the corpus medullare was not different, and the anterior lobe was significantly enlarged. Children with thoracic level lesions had smaller cerebellar volumes relative to those with lumbar/sacral lesions, who had smaller volumes compared to TD children. The reduction in cerebellar volume in the group with SBM represents not a change in linear scaling but rather a reconfiguration involving anterior lobe enlargement and posterior lobe reduction.

Keywords

Cerebellum; Volumetrics; Parcellation; Spina bifida; Chiari II

Introduction

Aberrant development of the cerebellum has been described in a range of neurodevelopmental disorders, including spina bifida meningomyelocele (SBM) [1], 22q deletion syndrome [2,3], Williams Syndrome [4], and autism [5–7]. Accounts of cerebellar anomalies in these disorders have been descriptive more often than quantitative, with both

Correspondence to: Jenifer Juranek, Jenifer.Juranek@uth.tmc.edu.

qualitative and quantitative studies categorizing the cerebellum based on historical clinical cerebellar signs (e.g., vermis vs. hemispheres) rather than parcellating it into subregions based on new clinical cerebellar maps [8] and current conceptualizations of cerebellar function [9–11]. Systematic comparisons of cerebellar structure across neurodevelopmental disorders are needed to better characterize the neuroanatomy of these disorders, to detail the anatomical connections between different regions of the cerebellum and cerebral cortex [12,13], and to sharpen hypotheses about cerebellar structure–function associations.

Abnormal development of the cerebellum is a central characteristic of SBM, the most common severely disabling congenital birth defect affecting the central nervous system in North America [14]. Although SBM is commonly identified by an open lesion on the spinal cord at birth, it also involves multiple anomalies of the brain. A key feature of SBM is the Chiari II malformation [15], a virtually ubiquitous deformity of the brainstem and cerebellum. The radiological presentation of the Chiari II varies [1], but is typically represented by a small posterior fossa and downward herniation of the cerebellum and hindbrain into the foramen of magnum. The vermis may tower over and above the tentorium, producing associated abnormalities of the midbrain, and the small posterior fossa produces mechanical abnormalities of the medulla. Cerebellar structures appear malformed, often with poor differentiation of the vermis and hemispheres.

Since Hans Chiari identified the cerebellar malformations in a series of papers in the 1890s [16,17], accounts of the cerebellum in Chiari II have been primarily descriptive. The few quantitative neuroimaging studies used simple subdivisions of cerebellar anatomy (midsagittal vs. lateral) on older generation MRI images, in which it was often difficult to identify anatomical landmarks in the malformed Chiari II cerebellum. Fletcher et al. [18] reported that children with SBM had reduced cerebellar volumes in lateral but not in medial cerebellum, and that the reduced cerebellar volumes were more strongly associated with thoracic level spinal lesions. Salman et al. [19] reported that, in SBM, mean posterior fossa area was significantly smaller, and mean vermis area was significantly larger, in vermis lobules I–V and VI–VII. These results are consistent with other quantitative studies of the supratentorial brain regions and white matter tracts in SBM, where, relative to controls, some brain structures are smaller and others are larger [20,21].

Newer methods for identifying the sub-regions of the cerebellum [22,23] provide a more finely grained understanding of cerebellar anatomy. Using a semi-automated approach, Pierson et al. [24] parcellated the cerebellum into four compartments based on tissue class (gray matter vs. white matter) and two prominent and delimiting fissures: the primary and horizontal fissures. The corpus medullare consists of the central white matter (WM) extending from the cerebellar peduncles to the richly branched folia in the lateral hemispheres, the primary fissure delineates the anterior from the posterior lobe, and the horizontal fissure further subdivides the posterior lobe into superior and inferior subdivisions. Cerebellar parcellations also enable the analysis of structure–function relations in neurodevelopmental disorders in a more theoretically cogent manner.

In this paper, we report volumetric analyses of regional variability of the cerebellum in children with SBM and typically developing controls to provide quantitative measures of cerebellar sub-regions that are structurally coherent and functionally significant. In our previous study of the cerebral cortex [21], cortical thickness in SBM followed a general gradient of being thicker in frontal areas and thinner in posterior regions relative to an age- and gender-matched healthy comparison group. Here, we investigate whether the hypoplastic cerebellum characteristic of SBM is smaller due to simple linear scaling or if some regional variability exists across the major subdivisions of the cerebellum. Upper (e.g., thoracic) rather than lower (e.g., lumbar/sacral) spinal lesion level has been associated with

increased supra- and subtentorial brain pathology [18], so we also evaluated whether level of spinal lesion is related to cerebellar volumes.

Methods

Participants

Children with SBM (*n*=30) were 7–16 years of age with shunted hydrocephalus, recruited from two primary sites in Houston, TX: the Spina Bifida Clinic at Texas Children's Hospital, and the Shriners Hospital for Children-Houston. All children were shunted within the first month of life, usually at the time of the repair of the spinal lesion. The children were medically stable at the time of the MRI. For the analyses, children were subdivided into those with upper (thoracic; *n*=10) vs. lower (lumbar, sacral; *n*=20) lesion levels based on models of neural tube closure and studies indicating genetic heterogeneity at this subdivision [25] and to evaluate whether cerebellar volumes vary by lesion level [18]. The comparison group of typically developing (TD) children was recruited from the community. The TD children had no history or evidence of neurological or neurodevelopmental disorder based on parental reports and assessments of cognitive functions.

Table 1 provides age, gender, ethnicity, and specific characteristics associated with SBM by lesion level. Some of these variables are known to influence brain development (e.g., age, sex) and so we used these as covariates. In addition, children in the TD group were younger, and a greater proportion were female, further justifying use of these covariates. In all groups, children of Hispanic origin were overrepresented, but consistent with the demographics of the southwestern recruitment city [18]. Among children with SBM, all but one participant had difficulties with ambulation, with more children in the upper spinal lesion group restricted to a wheelchair. All but three participants with SBM had at least one shunt revision, though only three had more than five revisions. Although not directly relevant to the study, Table 1 also presents the composite IQ score from the Stanford-Binet intelligence Test-IV [26], illustrating that this cohort has intellectual functions in the low average to average range, typical for children with SBM; more generally, this cohort is similar to the much larger cohort [18].

MRI Acquisition

High-resolution coronal brain MR images were acquired on a Philips 3T scanner with SENSE (Sensitivity Encoding) technology. After a conventional scout sequence, three-dimensional T1- and T2-weighted sequences were performed to obtain whole brain coverage. Acquisition parameters of the T1-weighted 3D turbo fast echo sequence were as follows: TR/TE=6.5–6.7/3.04–3.14 ms; flip angle=8°; square field-of-view=24 cm; matrix=256×256; slice thickness=1.5 mm; in-plane pixel dimensions (*x*, *y*)=0.94, 0.94; number of excitations (NEX)=2. Acquisition parameters of the T2-weighted 3D turbo spin echo sequence were as follows: TR/TE=80/5,000 ms; flip angle=90°; square field-of-view= 24 cm; matrix=256×256; slice thickness=1.5 mm; in-plane pixel dimensions (*x*, *y*)=0.94,0.94; NEX=1.

MR Image Analysis

Using BET [27,28] (Brain Extraction Tool v2.1) within FSLv4.0.4 software (http://www.fmrib.ox.ac.uk/fsl/), brain and non-brain areas were automatically identified, a brain mask generated, and brain components (e.g., GM, WM, and CSF) were extracted from the MR image (both T1- and T2-weighted image sets) for each subject. Subsequently, the outputs of BET for the T1 and the T2 image sets were verified for each subject using FSLView v3.0 and co-registered using a rigid body, six DOF model within FLIRT (FMRIB's Linear Image Registration Tool v5.4.2) using the correlation ratio cost function

and tri-linear interpolation options [29,30]. The co-registration was verified by reviewing the output in FSLView. FAST (FMRIB's Automated Segmentation Tool v3.53) was used to generate an intensity-based, three-class binary segmentation of the brain into CSF, GM, or WM from the co-registered T1- and T2-weighted image sets for each subject [31]. Partial volume maps for each segmentation class were also generated using the FAST utility for subsequent quantitative volumetric analyses.

Cerebellar Parcellation Units

A four-compartment model (one WM and three principally GM) was used to parcellate the cerebellum into the following regions: corpus medullare, anterior lobe, superior–posterior lobe, and inferior–posterior lobe. Consistent with boundary delineations described by Pierson et al. [24], each cerebellar parcellation unit was defined according to the following anatomical features: (1) corpus medullare: central white matter and output nuclei; (2) anterior lobe: lobules I–V, bounded by the most posterior point of the fourth ventricle, corpus medullare, and primary fissure; (3) superior–posterior lobe: lobe VI and crus I of VIIA, bounded by the primary fissure, corpus medullare, and horizontal fissure; and (4) inferior–posterior lobe: crus II of VIIA, VIIB, VIII, IX, and X, bounded by the most posterior point of the fourth ventricle, corpus medullare, and horizontal fissure. Although localization of anatomical landmarks in each individual brain was guided by the cerebellum atlas published by Schmahmann et al. [32], inter-individual uniqueness in cerebellar topography (e.g., fissures and lobes) was preserved because spatial transformations to a standardized template were not implemented.

Co-localization of Anatomical Landmarks and Manual Fissure Tracings in Cardinal Planes

As shown in Fig. 1, manually delineated fissure lines were used to mark the course of both the primary and horizontal fissures. Each fissure line was principally drawn in the plane that optimized our ability to follow the entire trajectory of each fissure (e.g., sagittal plane for horizontal fissure and para-sagittal and axial planes for primary fissure). Each fissure marker was readily visible in all three cardinal planes, independent of the plane selected for tracing. Subsequently, auxiliary fissure markers were added in complementary viewing planes to facilitate corroboration of fissure location before delineating boundaries of cerebellar parcellation units. Each parcellation unit label was assigned to a new unique mask overlying the T1-weighted image set. While the fissure lines provided delimiting boundaries between parcellation units, the multi-weighted and multi-channel segmentation results defined the GM/CSF border around the exterior edge of the cerebellum.

Statistical Analyses

The primary model was a repeated-measures ANOVA with a single between-subjects factor (group) with three levels (SBM upper level lesions, SBM lower level lesions, TD) and a single within-subjects factor (cerebellar region) with four levels (e.g., corpus medullare, anterior, inferior–posterior, and superior–posterior), with age and sex (and their interactions) evaluated as covariates. Initial models were run on absolute volumes comparing TD and the two SBM subgroups which were classified according to spinal lesion level. In performing these analyses, we also considered the role of one individual per group with the most divergently small cerebellar volumes. By way of follow-up, we then evaluated individual compartmental volumes relative to total cerebellum volume. Because the relative volumes summed to 1, the relative volumes were run in univariate fashion. Finally, we also evaluated the extent to which the parcellation of the posterior lobe into separate superior and inferior segments (vs. pooling both superior and inferior subdivisions together into a single composite structure) altered results. The follow-up analyses (on relative values and posterior lobe sub-parcellation) are reported only in the context of their relation to the primary analyses.

Results

Covariates and Outliers

Distributional analyses suggested that compartmental volumes were generally normal in their distribution within and across the TD group and two SBM subgroups (e.g., SBM upper level lesions and SBM lower level lesions). We evaluated two covariates, age and sex, with respect to group differences in cerebellar volumes, given the demonstrated developmental impact of these variables with regard to the cerebellum [33]. Although the groups differed in their proportion of age and sex, these variables were not strongly related to cerebellar volumes in this sample. In the whole sample, age was related variably to the absolute or relative (see below) volumes of compartments evaluated (range $|r|$= 0.00 to 0.32, median r=0.15). Sex was unrelated to cerebellum volumes (absolute or relative) in the sample as a whole (all p>0.05). Although we evaluated models with and without these variables and their interactions with group and/or cerebellar region, and also with and without the participants with the smallest within-group cerebellums, noted above, these did not substantively alter results of the absolute volumes. The one exception was a between-subjects interaction between age, sex, and group that did not vary across individual cerebellar compartments, $F(8,44)= 2.96$, p=0.0098. Follow-ups using the total cerebellar volume by sex revealed no age by group interaction on total cerebellar volumes for girls, p>0.05, but an age by group interaction for boys, $F(2,23)=7.99$, p<0.003, with the relation between age and cerebellum volumes stronger for SBM participants with lower level lesions relative to the other two groups. These results, however, were dependent on the individual with SBM with the smallest overall cerebellar volume, without whom the interaction was not significant in either the boys or the sample as a whole. Therefore, for all subsequent analyses, both covariates were trimmed from the models, and all participants were included.

Absolute Volumes

As shown in Fig. 2, the three groups differed significantly in total cerebellum volume [$F(2,34)=11.04$; p=0.0002]. Follow-up indicated that the SBM group with lower level lesions had volumes that were reduced by 20% [p=0.0049], and the SBM group with upper level lesions had volumes reduced by 43% [p=0.0001], relative to the TD group; furthermore, SBM participants with upper level lesions had volumes reduced by 20% relative to those with lower level lesions [p=0.0149].

Across the three compartments (e.g., corpus medullare and anterior and posterior lobes), there was an interaction of cerebellar compartment and group [Wilks λ=0.461, $F(4,66)=7.80$; p=0.0001]. Follow-up revealed that for the corpus medullare, the TD group had the largest volumes, relative to both SBM subgroups: lower level lesions [p= 0.0118] and upper level lesions [p=0.0003]. The SBM group with lower level lesions had larger volumes than the SBM group with upper level lesions [p=0.0376]. For the anterior lobe, the SBM subgroups did not differ from one another, though both the SBM subgroups, upper level lesions [p=0.0259] and lower level lesions [p=0.0493], had larger volumes relative to the TD group. The pattern for posterior cerebellar volumes mimicked that of the medullare, with the TD group having the largest volumes, relative to both SBM subgroups: lower level lesions [p=0.0012] and upper level lesions [p=0.0001]. SBM participants with lower level lesions had larger volumes than SBM participants with upper level lesions [p=0.0076].

Separate analyses were conducted within the posterior lobe, subdividing this into superior and inferior portions. There was an interaction of posterior subdivision and group [Wilks λ =0.569, $F(2,34)=12.85$; p=0.0001]. Follow-up revealed that for the inferior segment, the TD group had the largest volumes, relative to both SBM subgroups: lower level lesions [p=0.0001] and upper level lesions [p= 0.0001]. SBM participants with lower level lesions

had larger volumes than SBM participants with upper level lesions as well [p=0.0088]. In contrast, for the superior segment, SBM participants with upper level lesions had smaller volumes relative to both the SBM lower level lesions group [p=0.0232] as well as TD [p=0.0026]; the latter two groups did not differ from one another. Given this pattern, subsequent analyses utilized all four cerebellar compartments.

Relative Volumes

As shown in Table 2, within-group variability of total volumes was more extensively distributed in the group with SBM relative to the fairly homogeneous values observed in the TD group. Therefore, we corrected for individual differences in total cerebellum size by calculating proportionate ratios of each compartment's volume relative to total cerebellum volume (see Fig. 3). These relative volumes for each compartment were then used in all subsequent analyses. Table 2 shows that the standard deviations of means in the TD group were nearly half as variable as participants with SBM in each region of the cerebellum, which somewhat mitigates the effects of a relatively small number of participants in the TD group.

Using univariate analyses, SBM participants with upper lesion levels, lower lesion levels, and TD groups did not differ from one another in the corpus medullare fraction [F(2,34)=0.10; p=0.9049]. In terms of the posterior lobe fraction, SBM participants with upper lesion levels, lower lesion levels, and TD did not differ from one another for the superior section [F(2,34)=2.75; p=0.0785], but did for the inferior section [F(2,34)=18.32; p=0.0001]. As shown in Fig. 4, the TD group had the largest proportion relative to both SBM subgroups (both p=0.0001); in addition, the SBM group with lower level lesions had a larger proportion relative to the SBM group with upper level lesions (p=0.0354). Participants in the three groups also differed from one another in anterior fractions [F(2,34)=15.47; p=0.0001]. SBM participants with upper level lesions had a larger anterior fraction than SBM participants with lower level lesions (p=0.0009) and TD participants (p=0.0001); furthermore, SBM participants with lower level lesions also had a larger anterior fraction relative to the TD group (p=0.0059).

Discussion

In neurodevelopmental disorders, cerebral and cerebellar volumes are often significantly different from typically developing controls. The assumption that differences in brain volumes always involve reductions has been challenged by recent work showing both greater and lesser brain volumes [21]. In studying regional cerebellar volumes in SBM, the present paper contributes to specifying how subtentorial brain volumes represent an altered regional configuration in this disorder. The data bear on a number of issues: how SBM and TD groups differ in absolute and proportional cerebellar volumes; the putative scaling of cerebellar regional development; the possible functional significance of between-group cerebellar volume differences and within-group volume variability; and the broader question of whether the cerebellar profile in SBM is distinctive compared to that in other neurodevelopmental disorders with abnormal cerebellar development.

Consistent with a previous report by Fletcher et al. [18], total cerebellar volume is substantially reduced in SBM with the Chiari II malformation. Our volumetric analyses identified a 25% reduction in total cerebellum volume in participants with the Chiari II, differences that were larger in children with SBM and upper level spinal lesions. However, not all regions of the cerebellum were comparably reduced in the group with SBM. In both relative and absolute volumes of the anterior lobe, the group with SBM demonstrated significant enlargement of this region, despite an overall reduction in total cerebellar volume. In contrast, the absolute corpus medullare volumes and the absolute and

proportional posterior lobe volumes were significantly reduced in the group with SBM. Thus, the overall reduction in absolute cerebellar volume in the SBM group represents reduced WM of the corpus medullare and the posterior lobe.

The posterior lobe and corpus medullare are both scaled linearly downward with each other by 25%, suggesting that developmentally regulated processes underlying volumetric ratios in these two compartments might be coupled. Unlike the posterior lobe, corrected values of the corpus medullare (e.g., for total cerebellar volume), reflected proportionately “normal” values (e.g., 14% of total). Furthermore, unlike previous reports of GM in the lateral hemispheres [18], the corpus medullare was not affected by lesion level of the neural tube defect as reflected by the proportionately “normal” value identical in both upper and lower lesion subgroups with SBM. These findings indicate a non-linear scaling of functionally relevant regions of the cerebellum in SBM in both upper and lower level spinal lesions. Of interest, this scaling is not only non-linear, but also somewhat different from the available descriptions of typical longitudinal cerebellar development, in which the inferior superior and inferior superior regions are more strongly coupled to each other than is either to other parts of the cerebellum [33].

Quantifying regional cerebellar volumes in SBM provides benchmarks for comparing cerebellar development across neurodevelopmental disorders. In early MRI studies of Williams Syndrome, Jernigan et al. [34] reported reduced cerebral volume but well-preserved total cerebellar volume, including enlarged vermal lobules. Early MRI studies of autism identified reduced vermal lobules VI–VII [5,7,35]. 22q11.2 deletion syndrome provides an interesting contrast to SBM in cerebellar volume configuration. Relative to controls, cerebellar volumes in 22q11.2 deletion syndrome are reduced [36], particularly in midsagittal vermal lobules VI–VII [3], and the anterior cerebellum is hypoplastic [2]. Further cross-disorder cerebellar parcellation studies using the same MRI methodology, definitions of cerebellar regions, and volumetric analyses and parameters are necessary to decide whether the absolutely and proportionally enhanced anterior cerebellum in SBM is a feature of cerebellar development not shared by other neurodevelopmental disorders.

In severe cerebellar malformations including Dandy-Walker, Joubert syndrome, and pontocerebellar hypoplasia, the orchestrated processes underlying hindbrain development in utero are either disrupted or poorly timed [37,38]. The orchestration of cerebellar development in Chiari II, it appears, is quite complex, involving a combination of regional volumetric reduction and enlargement. In addition, continued associations of different quantitative brain indices with lesion level implies that different mechanisms may be involved for upper and lower spinal lesions. Spinal lesion level is related to differences in the unfolding of the neural tube [39] and is a marker for genetic variability [25]. Children with thoracic level lesions have more severe brain dysmorphology and quantitatively different cerebellar volumes, accounting for their significantly lower global cognitive outcome [18].

Broadly, the anterior lobe of the cerebellum is concerned with motor function, the inferior (by virtue of its connections with prefrontal and parietal cortices) with cognitive function [41]. The posterior cerebellar lobe is part of the “cognitive cerebellum” [41], including an executive network that includes the primary motor cortex, thalamus, and striatum.

Individuals with SBM have a range of deficits in motor strength and speed [42–44] and dynamic motor regulation [42–51]. Nevertheless, they have normal motor learning and adaptation: They can adapt saccades to backward target displacement [19], reach to prism-distorted visual input [52]; learn to draw a shape from an image in a mirror [53]; and adapt ballistic arm movement to changes in relation between movement and vision [54]. It is not

clear whether the enhanced anterior cerebellum volume plays a role in either preserved or impaired motor functions in SBM. Children and adults with SBM have mild forms of ataxic dysarthria [55] which might reflect their attenuated posterior cerebellar development (lobule VI of the posterior cerebellum has been suggested to instantiate internal models of articulation) [56]. Variation in regional cerebellar size may have functional significance for eye movements. Ocular motor function in individuals with SBM and an expanded midsagittal vermis is comparable to that of controls and better than that in individuals with SBM and a normal, non-expanded midsagittal vermis [57]. Our ongoing studies are investigating the functional significance of anomalous cerebellar development in SBM.

Conclusion

Regional volumetric analyses of the cerebellum in children with SBM and TD children showed that total cerebellar volume was significantly reduced in the SBM group relative to the TD group and, further, within the cerebellum, the anterior lobe was enlarged and the posterior lobe reduced. While cerebellar development is atypical in SBM, it is not yet clear whether the cerebellar configuration described here is unique to this condition. And while regional cerebellar expansion has been associated with enhanced ocular motor function in SBM [57], the significance of the enlarged anterior cerebellar lobe remains to be established.

Acknowledgments

This work is funded by NIH grants P01-HD35946 awarded to JMF and R01-HD046609 awarded to Dr. Susan Landry.

References

1. Raybaud, C.; Miller, E. Radiological evaluation of myelomeningocele–Chiari II malformation. In: Ozek, M.; Cinalli, G.; Maixner, W., editors. Spina bifida: management and outcome. Springer; Milan: 2008. p. 111-142.
2. Bish JP, Pendyal A, Ding L, Ferrante H, Nguyen V, McDonald-McGinn D, et al. Specific cerebellar reductions in children with chromosome 22q11.2 deletion syndrome. Neurosci Lett 2006;399 (3): 245–248. [PubMed: 16517069]
3. Eliez S, Schmitt JE, White CD, Wellis VG, Reiss AL. A quantitative MRI study of posterior fossa development in velocardiofacial syndrome. Biol Psychiatry 2001;49(6):540–546. [PubMed: 11257239]
4. Jones W, Hesselink J, Courchesne E, Duncan T, Matsuda K, Bellugi U. Cerebellar abnormalities in infants and toddlers with Williams syndrome. Dev Med Child Neurol 2002;44(10):688–694. [PubMed: 12418794]
5. Piven JMD, Saliba KMD, Bailey JBS, Arndt SP. An MRI study of autism: the cerebellum revisited. Neurology 1997;49(2):546–551. [PubMed: 9270594]
6. Courchesne E, Yeung-Courchesne R, Press G, Hesselink J, Jernigan T. Hypoplasia of cerebellar vermal lobules VI and VII in autism. N Engl J Med 1988;318(21):1349–1354. [PubMed: 3367935]
7. Filipek PA. Quantitative magnetic resonance imaging in autism: the cerebellar vermis. Curr Opin Neurol 1995;8(2):134–138. [PubMed: 7620587]
8. Apps R, Hawkes R. Cerebellar cortical organization: a one-map hypothesis. Nat Rev Neurosci 2009;10(9):670–681. [PubMed: 19693030]
9. Schmahmann JD. From movement to thought: anatomic substrates of the cerebellar contribution to cognitive processing. Hum Brain Mapp 1996;4(3):174–198. [PubMed: 20408197]
10. Schmahmann JD. Disorders of the cerebellum: ataxia, dysmetria of thought, and the cerebellar cognitive affective syndrome. J Neuropsychiatry Clin Neurosci 2004;16(3):367–378. [PubMed: 15377747]
11. Schmahmann JD, Sherman JC. The cerebellar cognitive affective syndrome. Brain 1998;121(4): 561–579. [PubMed: 9577385]

12. Kelly RM, Strick PL. Cerebellar loops with motor cortex and prefrontal cortex of a nonhuman primate. J Neurosci 2003;23 (23):8432–8444. [PubMed: 12968006]
13. Lu X, Miyachi S, Ito Y, Nambu A, Takada M. Topographic distribution of output neurons in cerebellar nuclei and cortex to somatotopic map of primary motor cortex. Eur J NeuroSci 2007;25 (8):2374–2382. [PubMed: 17445235]
14. Detrait ER, George TM, Etchevers HC, Gilbert JR, Vekemans M, Speer MC. Human neural tube defects: developmental biology, epidemiology, and genetics. Neurotoxicol Teratol 2006;27 (3): 515–524. [PubMed: 15939212]
15. Barkovich, J. Pediatric neuroimaging. 4. Lippincott, Williams & Wilkins; Philadelphia: 2005.
16. Koehler PJ. Chiari's description of cerebellar ectopy (1891). J Neurosurg 1991;75(5):823–826. [PubMed: 1919713]
17. Loukas M, Noordeh N, Shoja M, Pugh J, Oakes W, Tubbs R. Hans Chiari (1851–1916). Childs Nerv Syst 2008;24(3):407–409. [PubMed: 18066558]
18. Fletcher JM, Copeland K, Frederick JA, Blaser SE, Kramer LA, Northrup H, et al. Spinal lesion level in spina bifida: a source of neural and cognitive heterogeneity. J Neurosurg: Pediatrics 2005;102(3):268–279.
19. Salman MS, Blaser S, Sharpe J, Dennis M. Cerebellar vermis morphology in children with spina bifida and Chiari type II malformation. Childs Nerv Syst 2006;22(4):385–393. [PubMed: 16374591]
20. Hasan K, Eluvathingal T, Kramer L, Ewing-Cobbs L, Dennis M, Fletcher J. White matter microstructural abnormalities in children with spina bifida myelomeningocele and hydrocephalus: a diffusion tensor tractography study of the association pathways. J Magn Reson Imaging 2008;27(4):700–709. [PubMed: 18302204]
21. Juranek J, Fletcher JM, Hasan KM, Breier JI, Cirino PT, Pazo-Alvarez P, et al. Neocortical reorganization in spina bifida. NeuroImage 2008;40(4):1516–1522. [PubMed: 18337124]
22. Makris N, Hodge SM, Haselgrove C, Kennedy DN, Dale A, Fischl B, et al. Human cerebellum: surface-assisted cortical parcellation and volumetry with magnetic resonance imaging. J Cogn Neurosci 2003;15(4):584–599. [PubMed: 12803969]
23. Makris N, Schlerf JE, Hodge SM, Haselgrove C, Albaugh MD, Seidman LJ, et al. MRI-based surface-assisted parcellation of human cerebellar cortex: an anatomically specified method with estimate of reliability. NeuroImage 2005;25(4):1146–1160. [PubMed: 15850732]
24. Pierson R, Corson PW, Sears LL, Alicata D, Magnotta V, O'Leary D, et al. Manual and semiautomated measurement of cerebellar subregions on mr images. NeuroImage 2002;17(1):61–76. [PubMed: 12482068]
25. Volcik K, Blanton S, Tyerman G, Jong S, Rott E, Page T, et al. Methylenetetrahydrofolate reductase and spina bifida: evaluation of level of defect and maternal genotypic risk in Hispanics. Am J Med Genet 2000;95(1):21–27. [PubMed: 11074490]
26. Thorndike, RL.; Hagen, EP.; Sattler, JM. Guide for Administering and Scoring. 4. Chicago: The Riverside Publishing Company; 1986. The Stanford-Binet Intelligence Scale.
27. Jenkinson, M.; Pechaud, M.; Smith, S. BET2: MR-based estimation of brain, skull and scalp surfaces. Human Brain Mapping; Eleventh Annual Meeting; 2005.
28. Smith S. Fast robust automated brain extraction. Hum Brain Mapp 2002;17(3):143–155. [PubMed: 12391568]
29. Jenkinson M, Bannister P, Brady M, Smith S. Improved optimization for the robust and accurate linear registration and motion correction of brain images. NeuroImage 2002;17(2):825–841. [PubMed: 12377157]
30. Jenkinson M, Smith S. A global optimisation method for robust affine registration of brain images. Med Image Anal 2001;5 (2):143–156. [PubMed: 11516708]
31. Zhang Y, Brady M, Smith S. Segmentation of brain MR images through a hidden Markov random field model and the expectation maximization algorithm. IEEE Trans Med Imag 2001;20(1):45–57.
32. Schmahmann, JD.; Doyon, J.; Toga, A.; Petrides, M.; Evans, A. MRI atlas of the human cerebellum. Academic; San Diego: 2000.

33. Tiemeier H, Lenroot RK, Greenstein DK, Tran L, Pierson R, Giedd JN. Cerebellum development during childhood and adolescence: a longitudinal morphometric MRI study. NeuroImage 2010;49 (1):63–70. [PubMed: 19683586]
34. Jernigan T, Bellugi U. Anomalous brain morphology on magnetic resonance images in Williams syndrome and Down syndrome. Arch Neurol 1990;47(5):529–533. [PubMed: 2139774]
35. Courchesne E, Karns CM, Davis HR, Ziccardi R, Carper RA, Tigue ZD, et al. Unusual brain growth patterns in early life in patients with autistic disorder: an MRI study. Neurology 2001;57(2):245–254. [PubMed: 11468308]
36. Eliez S, Schmitt JE, White CD, Reiss AL. Children and adolescents with velocardiofacial syndrome: a volumetric MRI study. Am J Psychiatry 2000;157(3):409–415. [PubMed: 10698817]
37. Aldinger KA, Elsen GE, Prince VE, Millen KJ. Model organisms inform the search for the genes and developmental pathology underlying malformations of the human hindbrain. Semin Pediatr Neurol 2009;16(3):155–163. [PubMed: 19778712]
38. ten Donkelaar HJ, Lammens M. Development of the human cerebellum and its disorders. Clin Perinatol 2009;36(3):513–530. [PubMed: 19732611]
39. Van Allen M, Kalousek D, Chernoff G, Juriloff D, Harris M, McGillivray B, et al. Evidence for multi-site closure of the neural tube in humans. Am J Med Genet 1993;47(5):723–743. [PubMed: 8267004]
40. Middleton FA, Strick PL. The cerebellum: an overview. Trends Neurosci 1998;21(9):367–369. [PubMed: 9735943]
41. Stoodley CJ, Schmahmann JD. The cerebellum and language: evidence from patients with cerebellar degeneration. Brain Lang 2009;110(3):149–153. [PubMed: 19664816]
42. Hetherington R, Dennis M. Motor function profile in children with early onset hydrocephalus. Dev Neuropsychol 1999;15(1):25–51.
43. Zeiner HK, Prigatano GP, Pollay M, Biscoe CB, Smith RV. Ocular motility, visual acuity and dysfunction of neuropsychological impairment in children with shunted uncomplicated hydrocephalus. Childs Nerv Syst 1985;1(2):115–122. [PubMed: 4005882]
44. Ziviani J, Hayes A, Chant D. Handwriting: a perceptual-motor disturbance in children with myelomeningocele. Occup Ther J Res 1990;10:12–26.
45. Jewell D, Fletcher J, Mahy C, Hetherington R, MacGregor D, Drake J, et al. Upper limb cerebellar motor function in children with spina bifida. Childs Nerv Syst 2009;26(1):67–73. [PubMed: 19823846]
46. Salman M, Sharpe J, Lillakas L, Steinbach M, Dennis M. Smooth ocular pursuit in Chiari type II malformation. Dev Med Child Neurol 2007;49(4):289–293. [PubMed: 17376140]
47. Wills K. Neuropsychological functioning in children with spina bifida and/or hydrocephalus. J Clin Child Psychol 1993;22(2):247–265.
48. Sandler A, Macias M, Brown T. The drawings of children with spina bifida: developmental correlations and interpretations. Eur J Pediatr Surg 1993;3(S1):25–27. [PubMed: 8130145]
49. Soare P, Raimondi A. Intellectual and perceptual-motor characteristics of treated myelomeningocele children. Am J Dis Child 1977;131(2):199–204. [PubMed: 319654]
50. Pearson A, Carr J, Hallwell M. The handwriting of children with spina bifida. Zeitschrift für Kinderchirurgie 1988;43(S2):40–42.
51. Fletcher, J.; Brookshire, B.; Bohan, T.; Brandt, M.; Davidson, K. Early hydrocephalus. In: Rourke, B., editor. Syndrome of nonverbal learning disabilities: neurodevelopmental manifestations. Guilford; New York: 1995. p. 206-238.
52. Colvin AN, Yeates KO, Enrile BG, Coury DL. Motor adaptation in children with myelomeningocele: comparison to children with ADHD and healthy siblings. J Int Neuropsychol Soc 2003;9(04):642–652. [PubMed: 12755176]
53. Edelstein KIM, Dennis M, Copeland KIM, Frederick JON, Francis D, Hetherington R, et al. Motor learning in children with spina bifida: dissociation between performance level and acquisition rate. J Int Neuropsychol Soc 2004;10(06):877–887. [PubMed: 15637778]
54. Dennis M, Jewell D, Edelstein KIM, Brandt ME, Hetherington R, Blaser SE, et al. Motor learning in children with spina bifida: intact learning and performance on a ballistic task. J Int Neuropsychol Soc 2006;12(05):598–608. [PubMed: 16961941]

55. Huber-Okrainec J, Dennis M, Brettschneider J, Spiegler BJ. Neuromotor speech deficits in children and adults with spina bifida and hydrocephalus. Brain Lang 2002;80(3):592–602. [PubMed: 11896659]

56. Callan D, Kawato M, Parsons L, Turner R. Speech and song: the role of the cerebellum. The Cerebellum 2007;6(4):321–327.

57. Salman M, Dennis M, Sharpe J. The cerebellar dysplasia of Chiari II malformation as revealed by eye movements. Can J Neurol Sci 2009;36:713–724. [PubMed: 19960749]

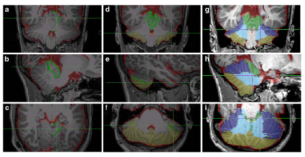

Fig. 1.
Cardinal views of T1-weighted images with CSF boundary information (*light red*) determined from co-registered T2-weighted images. **a**–**c** Parcellation of anterior lobe by utilizing manual guide traces for the primary fissure. **d–f** Parcellation of the posterior lobe in two subdivisions (e.g., posterior–inferior and posterior–superior) by manually delineating the horizontal fissure. **g**–**i** Inclusion of the corpus medullare with the other three parcels of the cerebellum

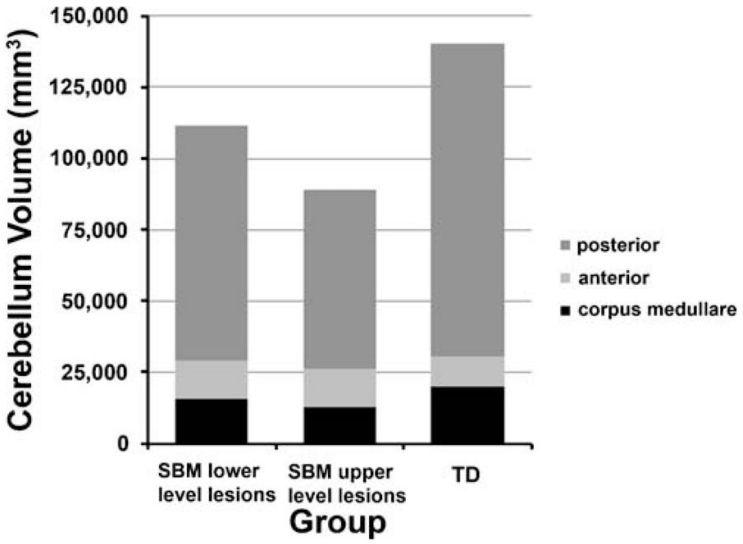

Fig. 2.

Group comparisons of average total cerebellum volumes (mm^3) displayed in stacked columns consisting of three principal compartments: corpus medullare, anterior lobe, and posterior lobe

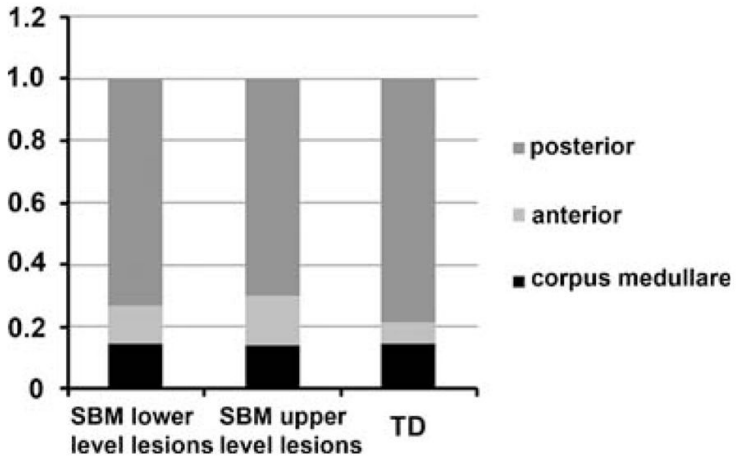

Fig. 3.

Group comparisons of three cerebellum compartments (e.g., corpus medullare, anterior lobe, and posterior lobe) expressed as percentage of total cerebellum volume

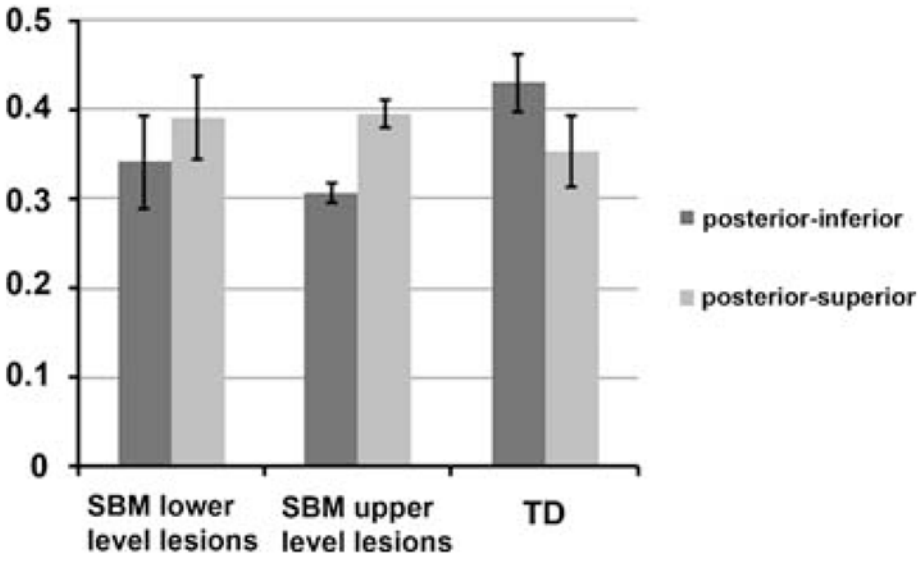

Fig. 4.

Group comparisons of inferior and superior subdivisions of the posterior lobe expressed as percentages of total cerebellum volume. *Error bars* reflect standard deviations of group means

Table 1

Demographic and medical characteristics of study participants

	Spina bifida myelomeningocele		Typically developing
	Thoracic lesion (upper level)	Lumbar/sacral lesion (lower level)	
n	10	20 (17 lumbar)	7
Age at MRI (M, SD)	12.72 (1.5)	13.60 (2.8)	10.37 (1.5)
Sex (M:F)	6:4	15:5	3:4
Handedness (R:L)	7:3	16:4	6:1
Ethnicity	5H; 5C	14H; 4AA; 2C	6H; 1C
Ambulatory status	2P; 8U	1N; 7I; 9P; 3U	–
Age at shunt (days)	10.30 (6.5)	9.65 (7.9)	–
Shunt revisions	6:<2; 3:2–4; 1:5–9	8:<2; 10:2–4; 1:5–9; 1:>9	–
FSIQ (M, SD)	83.9 (11.2)	85.7 (11.0)	105.3 (8.6)

H Hispanic, *AA* African American, *C* Caucasian, *N* normal, *I* independent, *P* partial, *U* unable, *FSIQ* Full Scale IQ

Table 2

Absolute cerebellar volume means, and corrected relative means, by compartment, for SBM upper level lesions (*n*=10) and SBM lower level lesions (*n*=20) and TD (*n*=7)

	Absolute volumes mm^3 (SD)			Relative volumes percentage (SD)		
	SBM upper level lesions	SBM lower level lesions	TD	SBM upper level lesions	SBM lower level lesions	TD
Corpus medullare	12,849.52 (4,346.33)	15,867.84 (3,574.29)	20,077.30 (2,177.44)	0.14 (0.01)	0.14 (0.01)	0.14 (0.01)
Anterior	14,009.02 (4,621.02)	13,203.70 (2,713.64)	10,350.07 (1,489.57)	0.16 (0.03)	0.12 (0.04)	0.07 (0.01)
Posterior–inferior	27,905.06 (8,709.46)	39,175.63 (12,189.50)	60,517.80 (6,009.06)	0.31 (0.01)	0.34 (0.05)	0.43 (0.03)
Posterior–superior	35,584.51 (10,487.11)	43,640.78 (8,608.96)	49,597.45 (5,830.41)	0.39 (0.02)	0.39 (0.05)	0.35 (0.04)